TÜBİTAK

Turkish Journal of Physics

http://journals.tubitak.gov.tr/physics/

Research Article

Turk J Phys
(2014) 38: 50 – 63

doi:10.3906/fiz-1210-10

Soret and Dufour effects on an MHD free convective flow through a channel bounded by a long wavy wall and a parallel flat wall

Nazibuddin AHMED[1,*], **Kalpana SARMA**[2], **Hiren DEKA**[2]
[1]Department of Mathematics, Gauhati University, Guwahati, India
[2]Department of Mathematics, Cotton College, Guwahati, India

Received: 24.10.2012 • **Accepted:** 03.06.2013 • **Published Online:** 17.01.2014 • **Printed:** 14.02.2014

Abstract: This paper presents Soret and Dufour effects on a 2-dimensional free convective magnetohydrodynamic (MHD) flow of a viscous incompressible and electrically conducting fluid through a channel bounded by a long vertical wavy wall and a parallel flat wall. A uniform magnetic field is assumed to be applied perpendicular to the flat wall. Governing equations of the fluid flow and heat and mass transfer are solved analytically subject to the relevant boundary conditions. It is assumed that the solution consists of 2 parts, a mean part and a perturbed part. The long wave approximation has been used to obtain the solution of the perturbed part. The perturbed part of the solution is the contribution from the waviness of the wall. The expressions for zeroth- and first-order velocity, temperature, concentration, skin friction, and the rate of heat and mass transfer at the walls are obtained. Some of the results indicating the influence of Soret and Dufour effects on the above fields are presented graphically.

Key words: Magnetohydrodynamic, free convective, Soret effect, Dufour effect

2010 Subject Classification: 76W 05

1. Introduction

The incompressible boundary layer flow over a wavy wall has importance because of its application in different areas such as cross-hatching on ablative surfaces, transpiration cooling of reentry vehicles and rocket boosters, and film vaporization in combustion chambers. Lukodius et a. [1] made a linear analysis of compressible boundary layer flows over a wavy wall. The Rayleigh problem for wavy wall was studied by Shankar and Sinha [2]. They arrived at the interesting conclusion that at low Reynolds numbers the waviness of the wall quickly ceases to be of importance as the liquid is dragged along by the wall, while at large Reynolds numbers the effects of viscosity are confined to a thin layer close to the wall and a known potential solution emerges in time. The analysis of the effect of small-amplitude wall waviness upon the stability of the laminar boundary layer was made by Lessen and Gangwani [3]. Vajravelu and Sastri [4] made an analysis of the free convective heat transfer in a viscous incompressible fluid between a long vertical wavy wall and a parallel flat wall. Furthermore, they extended their work for vertical wavy channels. Rao and Sastri [5] studied the work of Vajravelu and Sastri [6] for viscous heating effects when the fluid properties are constants and variables. Again Rao [7] reinvestigated the problem of Rao and Sastri [5] for channels that are of different wave numbers. Das and Ahmed [8] studied the free convective magnetohydrodynamic (MHD) flow and heat transfer in a viscous incompressible fluid confined

*Correspondence: saheel_nazib@yahoo.com

between a long vertical wavy wall and a parallel flat wall. In the above mentioned works, the diffusion–thermo (Dufour) and the thermal–diffusion (Soret) terms were not taken into account in the energy and concentration equations, respectively. However, when the heat and mass transfers occur simultaneously in a moving fluid, the relations between the fluxes and driving potentials are of a more intricate nature. It is found that a heat flux can be generated not only by temperature gradients but by composition gradients as well. The heat flux that occurs due to composition gradient is called the Dufour effect or diffusion–thermo effect. On the other hand, the flux of mass caused due to temperature gradient is known as the Soret effect or the thermal–diffusion effect. In general, the Soret and Dufour effects are of a smaller order of magnitude than the effects described in Fourier's or Fick's law and are often neglected in heat and mass transfer processes. Though these effects are quite small, the devices can be arranged to produce very steep temperature and concentration gradients so that the separation of components in mixtures are affected. Eckert and Drake [9] emphasized that the Soret effect assumes significance in cases concerning isotope separation, and in mixtures between gases with very light molecular weight (H_2, H_e) and for medium molecular weight (N_2, air), the Dufour effect is found to be of considerable magnitude such that it cannot be ignored. Following Eckert and Drake's work, several other investigators carried out model studies on the Soret and Dufour effects in different heat and mass transfer problems. Some of them are Dursunkaya and Worek [10], Kafoussias and Williams [11], Sattar and Alam [12], Alam et al. [13], Raju et al. [14] and Srinivasacharya and RamReddy [15–18]. Due to the importance of the thermal–diffusion and diffusion–thermo effects on the heat and mass transfer-related problems, we propose in this paper to study the Soret and Dufour effects in free convective MHD flow of a viscous incompressible fluid through a channel bounded by a long vertical wavy wall and a parallel flat wall.

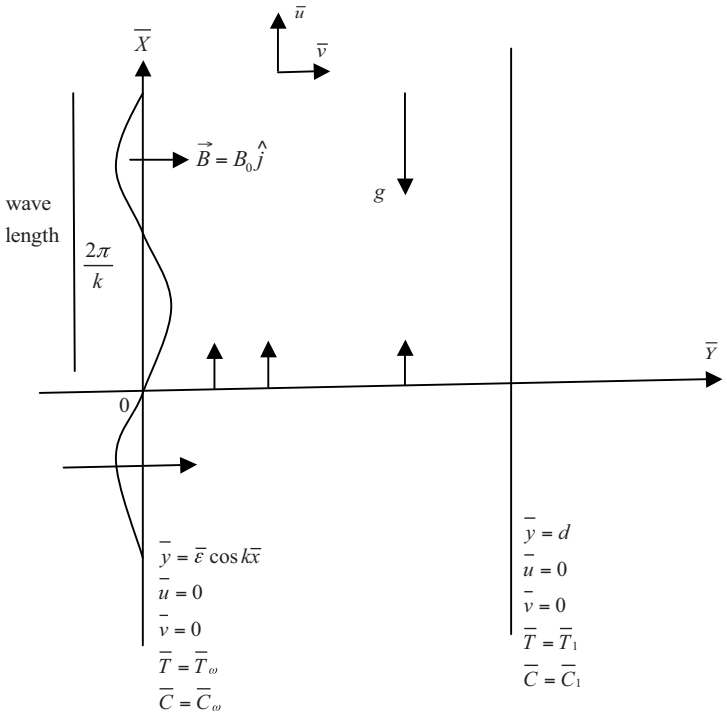

Flow configuration

2. Basic equations

The 2-dimensional steady laminar free convective MHD flow along the vertical channel is considered here. The $\bar{x}$-axis is taken vertically upwards and parallel to the flat wall and the $\bar{y}$-axis is perpendicular to it. The wavy wall is represented by $\bar{y} = \bar{\varepsilon}\cos k\bar{x}$ and the flat wall is by $\bar{y} = d$. $\bar{T}_\omega$ and $\bar{\bar{T}}_1$ are the constant temperatures of the wavy wall and the flat wall, respectively.

Our investigation is restricted to the following assumptions:

(i) All the fluid properties except the density in the buoyancy force term are constants. We intend to apply the Boussinesq approximation, and this requires the aforesaid assumption. It may be noted that free convection flows are actually buoyancy-driven flows arising out of small density differences in the fluid owing to the presence of temperature and species concentration gradients in the fluid. Thus, for free convective flows, the density in the buoyancy force term cannot remain constant; rather, it varies according to the temperature and the species concentration differences (gradients) in the fluid. This necessitates the use of Boussinesq approximation to the equation of state. Boussinesq approximations in free convection flows are common in nature (such as oceanic circulation), industry (such as dispersion of dense gas and fume ventilation), and building environments (such as natural ventilation and central heating). This approximation is reasonably precise for many convection flows and renders the mathematical calculations relatively simpler.

1. The viscous and magnetic dissipation of energy are negligible. The inclusion of the viscous energy dissipation term is necessary for high-speed flows. However, for free convection flows, the flow velocities are considerably small. Therefore, the viscous dissipative effects may be safely neglected. On the other hand, the magnetic dissipation (Joule heating effect) has relevance only when the fluid medium has a significantly high electrical conductivity. In the present problem, we assume the fluid medium to possess low/moderate electrical conductivity. Thus, the magnetic dissipative effects may be omitted.

(ii) The volumetric heat source/sink term in the energy equation is constant. Hence, the heat source or sink is time-independent, i.e. constant. The presence of a heat source/sink is helpful in controlling the temperature field and the rate of heat transfer. This application is undeniably vital to engineering applications and technology concerning transport phenomena.

(iii) The magnetic Reynolds number is small enough to neglect the induced magnetic field. Thus, the applied magnetic field has relatively low strength, i.e. the applied magnetic field is not too strong. Consequently, the effect of the induced magnetic field may be neglected.

(iv) The wave length of the wavy wall, which is proportional to 1/k, is large.

Under the foregoing assumptions, the equations that govern the 2-dimensional steady laminar free convective MHD flow and heat transfer in a viscous incompressible fluid occupying the channel are given below.

The momentum equations:

$$\rho\left[\bar{u}\frac{\partial\bar{u}}{\partial\bar{x}} + \bar{v}\frac{\partial\bar{u}}{\partial\bar{y}}\right] = -\frac{\partial\bar{p}}{\partial\bar{x}} + \mu\left(\frac{\partial^2\bar{u}}{\partial\bar{x}^2} + \frac{\partial^2\bar{u}}{\partial\bar{y}^2}\right) - \rho g - \sigma\bar{B}^2\bar{u} \tag{1}$$

$$\rho\left[\bar{u}\frac{\partial\bar{v}}{\partial\bar{x}} + \bar{v}\frac{\partial\bar{v}}{\partial\bar{y}}\right] = -\frac{\partial\bar{p}}{\partial\bar{y}} + \mu\left(\frac{\partial^2\bar{u}}{\partial\bar{x}^2} + \frac{\partial^2\bar{v}}{\partial\bar{y}^2}\right) \tag{2}$$

The continuity equation:

$$\frac{\partial \bar{u}}{\partial \bar{x}} + \frac{\partial \bar{v}}{\partial \bar{y}} = 0 \tag{3}$$

The energy equation:

$$\rho C_p \left[\bar{u}\frac{\partial \bar{T}}{\partial \bar{x}} + \bar{v}\frac{\partial \bar{T}}{\partial \bar{y}}\right] = k\left(\frac{\partial^2 \bar{T}}{\partial \bar{x}^2} + \frac{\partial^2 \bar{T}}{\partial \bar{y}^2}\right) + \frac{\rho D_M K_T}{C_s}\left(\frac{\partial^2 \bar{C}}{\partial \bar{x}^2} + \frac{\partial^2 \bar{C}}{\partial \bar{y}^2}\right) + Q \tag{4}$$

The species continuity equation:

$$\bar{u}\frac{\partial \bar{C}}{\partial \bar{x}} + \bar{v}\frac{\partial \bar{C}}{\partial \bar{y}} = D_M\left(\frac{\partial^2 \bar{C}}{\partial \bar{x}^2} + \frac{\partial^2 \bar{C}}{\partial \bar{y}^2}\right) + \frac{D_M K_T}{T_m}\left(\frac{\partial^2 \bar{T}}{\partial \bar{x}^2} + \frac{\partial^2 \bar{T}}{\partial \bar{y}^2}\right) \tag{5}$$

In static conditions, Eq. (1) takes the following form.

$$0 = -\frac{\partial \bar{p}_s}{\partial \bar{x}} - \rho_s g \tag{6}$$

Now Eqs. (1) through (6) yield the following.

$$\rho\left[\bar{u}\frac{\partial \bar{u}}{\partial \bar{x}} + \bar{v}\frac{\partial \bar{v}}{\partial \bar{y}}\right] = -\frac{\partial}{\partial \bar{x}}\left(\bar{p} - \bar{p}_s\right) + g\left(\rho_s - \rho\right) + \mu\left(\frac{\partial^2 \bar{u}}{\partial \bar{x}^2} + \frac{\partial^2 \bar{u}}{\partial \bar{y}^2}\right) - \sigma B^2 \bar{u} \tag{7a}$$

The equation of state is given by Boussinesq approximation:

$$\rho = \rho_s\left[1 - \beta\left(\bar{T} - \bar{T}_s\right) - \bar{\beta}\left(\bar{C} - \bar{C}_s\right)\right] \tag{7b}$$

Eqs. (7a) and (7b) together give:

$$\rho\left[\bar{u}\frac{\partial \bar{u}}{\partial \bar{x}} + \bar{v}\frac{\partial \bar{u}}{\partial \bar{y}}\right] = -\frac{\partial}{\partial \bar{x}}\left(\bar{p} - \bar{p}_s\right) + \rho g\left[\beta\left(\bar{T} - \bar{T}_s\right) + \bar{\beta}\left(\bar{C} - \bar{C}_s\right)\right] + \mu\left(\frac{\partial^2 \bar{u}}{\partial \bar{x}^2} + \frac{\partial^2 \bar{u}}{\partial \bar{y}^2}\right) - \sigma B^2 \bar{u} \tag{8}$$

The boundary conditions are:

$$\bar{y} = \bar{\varepsilon}\cos k\bar{x} : \bar{u} = 0, \bar{v} = 0, \bar{T} = \bar{T}_\omega, \bar{C} = \bar{C}_\omega \tag{9}$$

$$\bar{y} = d : \bar{u} = 0, \bar{v} = 0, \bar{T} = \bar{T}_1, \bar{C} = \bar{C}_1 \tag{10}$$

We define the following nondimensional quantities:

$$x = \frac{\bar{x}}{d}, y = \frac{\bar{y}}{d}, u = \frac{\bar{u}d}{\upsilon},\ \mathrm{v} = \frac{\bar{v}d}{\upsilon},\ p = \frac{\bar{p}d^2}{\rho\upsilon^2}, p_s = \frac{\bar{p}_s d^2}{\rho\upsilon^2}, \lambda = kd, \varepsilon = \frac{\bar{\varepsilon}}{d}, Pr = \frac{\mu C_p}{k},$$

$$Gr = \frac{d^3 g\beta\left(\bar{T}_\omega - \bar{T}_s\right)}{\upsilon^2}, Gm = \frac{d^3 g\bar{\beta}\left(\bar{C}_\omega - \bar{C}_s\right)}{\upsilon^2}, n = \frac{\bar{C}_1 - \bar{C}_s}{\bar{C}_\omega - \bar{C}_s},$$

$$Sr = \frac{D_M K_T\left(\bar{T}_\omega - \bar{T}_s\right)}{\upsilon T_m\left(\bar{C}_\omega - \bar{C}_s\right)}, Du = \frac{D_M K_T\left(\bar{C}_\omega - \bar{C}_s\right)}{\upsilon C_s C_p\left(\bar{T}_\omega - \bar{T}_s\right)}, Sc = \frac{\upsilon}{D_M},$$

$$M=\frac{\sigma B^2 d^2}{\rho \upsilon}, T=\frac{\bar{T}-\bar{T}_s}{\bar{T}_\omega-\bar{T}_s}, C=\frac{\bar{C}-\bar{C}_s}{\bar{C}_\omega-\bar{C}_s}, \alpha=\frac{Qd^2}{k\left(\bar{T}_\omega-\bar{T}_s\right)}, m=\frac{\bar{T}_1-\bar{T}_s}{\bar{T}_\omega-\bar{T}_s}$$

All physical variables and parameters are defined in the nomenclature section.

The governing equations in nondimensional form are follows.

$$u\frac{\partial u}{\partial x}+v\frac{\partial u}{\partial y}=-\frac{\partial\left(p-p_s\right)}{\partial x}+\frac{\partial^2 u}{\partial y^2}+\frac{\partial^2 u}{\partial x^2}+GrT+GmC-Mu \tag{11}$$

$$u\frac{\partial v}{\partial x}+v\frac{\partial v}{\partial y}=-\frac{\partial p}{\partial y}+\frac{\partial^2 v}{\partial x^2}+\frac{\partial^2 v}{\partial y^2} \tag{12}$$

$$\frac{\partial^2 T}{\partial x^2}+\frac{\partial^2 T}{\partial y^2}+PrDu\left(\frac{\partial^2 C}{\partial x^2}+\frac{\partial^2 C}{\partial y^2}\right)=Pr\left(u\frac{\partial T}{\partial x}+v\frac{\partial T}{\partial y}\right)-\alpha \tag{13}$$

$$\frac{1}{Sc}\left(\frac{\partial^2 C}{\partial x^2}+\frac{\partial^2 C}{\partial y^2}\right)+Sr\left(\frac{\partial^2 T}{\partial x^2}+\frac{\partial^2 T}{\partial y^2}\right)=u\frac{\partial C}{\partial x}+v\frac{\partial C}{\partial y} \tag{14}$$

$$\frac{\partial u}{\partial x}+\frac{\partial v}{\partial y}=0 \tag{15}$$

Their boundary conditions are:

$$u=0, v=0, T=1, C=1 \text{ at } y=\varepsilon\cos\lambda x \tag{16}$$

$$u=0, v=0, T=m, C=n \text{ at } y=1 \tag{17}$$

3. Method of solutions

In order to solve Eqs. (11) through (15), we assume u, v, p, T, and C as follows:

$$u\left(x,y\right)=u_0\left(y\right)+\varepsilon u_1\left(x,y\right)+\ldots\ldots\ldots\ldots \tag{18.1}$$

$$v\left(x,y\right)=\varepsilon v_1\left(x,y\right)+\ldots\ldots\ldots\ldots \tag{18.2}$$

$$p\left(x,y\right)=p_0\left(x\right)+\varepsilon p_1\left(x,y\right)+\ldots\ldots\ldots\ldots\ldots \tag{18.3}$$

$$T\left(x,y\right)=T_0\left(y\right)+\varepsilon T_1\left(x,y\right)+\ldots\ldots\ldots\ldots\ldots \tag{18.4}$$

$$C\left(x,y\right)=C_0\left(y\right)+\varepsilon C_1\left(x,y\right)+\ldots\ldots\ldots\ldots \tag{18.5}$$

Here the subscripts 0 and 1 denote respectively the corresponding zeroth- and first-order quantities.

By substituting the transformations from Eqs. (18.1) through (18.5) into Eqs. (11) through (15), and by equating the coefficients of ε^0, ε and neglecting the higher powers of ε and assuming $\frac{\partial}{\partial x}\left(p_0-p_s\right)=0$ (see [18]), we derive the following set of ordinary differential equations:

$$\frac{d^2 u_0}{dy^2}-Mu_0=-GrT_0-GmC_0 \tag{19}$$

$$\frac{d^2 T_0}{dy^2}+PrDu\frac{d^2 C_0}{dy^2}=-\alpha \tag{20}$$

$$\frac{d^2 C_0}{dy^2}+SrSc\frac{d^2 T_0}{dy^2}=0 \tag{21}$$

$$u_0\frac{\partial u_1}{\partial x}+v_1 u_0'=-\frac{\partial p_1}{\partial x}+\frac{\partial^2 u_1}{\partial y^2}+\frac{\partial^2 u_1}{\partial x^2}+GrT_1+GmC_1-Mu_1 \tag{22}$$

$$u_0\frac{\partial v_1}{\partial x}=-\frac{\partial p_1}{\partial y}+\frac{\partial^2 v_1}{\partial x^2}+\frac{\partial^2 v_1}{\partial y^2} \tag{23}$$

$$\frac{\partial u_1}{\partial x}+\frac{\partial v_1}{\partial y}=0 \tag{24}$$

$$\frac{\partial^2 T_1}{\partial x^2}+\frac{\partial^2 T_1}{\partial y^2}+PrDu\left[\frac{\partial^2 C_1}{\partial x^2}+\frac{\partial^2 C_1}{\partial y^2}\right]=Pr\left[u_0\frac{\partial T_1}{\partial x}+v_1T_0'\right] \tag{25}$$

$$\frac{1}{Sc}\left[\frac{\partial^2 C_1}{\partial x^2}+\frac{\partial^2 C_1}{\partial y^2}\right]+Sr\left[\frac{\partial^2 T_1}{\partial x^2}+\frac{\partial^2 T_1}{\partial y^2}\right]=u_0\frac{\partial C_1}{\partial x}+v_1C_0' \tag{26}$$

These are subject to the following boundary conditions:

$$u_0=0,T_0=1,C_0=1 \text{ at } y=0$$

$$u_0=0,T_0=m,C_0=n \text{ at } y=1 \tag{27}$$

$$u_1=-Re\left[u_0'(o)\,e^{i\lambda x}\right],v_1=0,T_1=-Re\left[T_0'(0)\,e^{i\lambda x}\right],C_1=-Re\left[C_0'(0)\,e^{i\lambda x}\right] \text{ at } y=0$$

$$u_1=0,v_1=0,T_1=0,C_1=0aty=1 \tag{28}$$

The solutions of the Eqs. (20), (21), and (19) subject to the boundary conditions of Eq. (27) are:

$$T_0=1+\left(m-1-\frac{\lambda_1}{2}\right)y+\frac{\lambda_1}{2}y^2 \tag{29}$$

$$C_0=-SrScT_0+1+SrSc+y\left\{(n-1)+(m-1)\,SrSc\right\} \tag{30}$$

$$u_0=A_6e^{\sqrt{M}y}+A_7e^{-\sqrt{M}y}-\frac{A_2}{M}y-\frac{A_3}{M}y^2-A_4 \tag{31}$$

Here, $\lambda_1=\frac{\alpha}{PrDuSrSc-1}$, $A_1=-Gr-Gm$, $A_2=-Gr\left(m-1-\frac{\lambda_1}{2}\right)+Gm\,(n-1)+\frac{GmSrSc\lambda_1}{2}$, $A_3=-\frac{Gr\lambda_1}{2}+GmSrSc\frac{\lambda_1}{2}$, $A_4=\frac{1}{M}\left(A_1+\frac{2A_3}{M}\right)$, $A_5=\frac{1}{M}\left(A_1+A_2+A_3+\frac{2A_3}{M}\right)$, $A_6=\frac{A_5-A_4e^{-\sqrt{M}}}{e^{\sqrt{M}}-e^{-\sqrt{M}}}$ and $A_7=\frac{A_4e^{\sqrt{M}}-A_5}{e^{\sqrt{M}}-e^{-\sqrt{M}}}$.

Now to get the solutions of the first-order equations, we introduce the stream function $\bar{\psi}_1$, defined by:

$$u_1=-\frac{\partial\bar{\psi}_1}{\partial y},v_1=\frac{\partial\bar{\psi}_1}{\partial x} \tag{32}$$

Upon elimination of p, Eqs. (22), (23), (25), and (26) yield:

$$u_0\left[\bar{\psi}_{1,xxy}+\bar{\psi}_{1,xxx}\right]-u_0''\bar{\psi}_{1,x}=\bar{\psi}_{1,yyyy}+2\bar{\psi}_{1,xxyy}+\bar{\psi}_{1,xxxx}-GrT_{1,y}-GmC_{1,y}-M\bar{\psi}_{1,yy} \tag{33}$$

$$T_{1,xx}+T_{1,yy}+PrDu\left[C_{1,xx}+C_{1,yy}\right]=Pr\left[u_0T_{1,x}+\bar{\psi}_{1,x}T_0'\right] \tag{34}$$

$$\frac{1}{Sc}\left[C_{1,xx}+C_{1,yy}\right]+Sr\left[T_{1,xx}+T_{1,yy}\right]=u_0C_{1,x}+\bar{\psi}_{1,x}C_0' \tag{35}$$

Consider the transformations $\bar{\psi}_1=e^{i\lambda x}\psi(y)$, $T_1=e^{i\lambda x}\theta(y)$ and $C_1=e^{i\lambda x}\phi(y)$.

Eqs. (33), (34), and (35) reduce to:

$$\psi^{iv}-\left[u_0\left(\psi''-\lambda^2\psi\right)\right]+i\lambda\psi u_0''-2\lambda^2\psi''-M\psi''+\lambda^4\psi=Gr\theta'+Gm\phi' \tag{36}$$

$$\theta'' - \theta\left(\lambda^2 + Pru_0 i\lambda\right) + PrDu\left(\phi'' - \lambda^2\phi\right) = Pri\lambda\psi T_0' \tag{37}$$

$$\frac{1}{Sc}\left[-\lambda^2\phi + \phi''\right] + Sr\left[-\lambda^2\theta + \theta''\right] = u_0 i\lambda\phi + i\lambda\psi\phi_o' \tag{38}$$

These are subject to the relevant boundary conditions:

$$\psi'(y) = u_0'(0), \psi(y) = 0, \theta(y) = T_0'(0), \phi(y) = -C_0'(0) \text{ at } y = 0 \tag{39}$$

$$\psi'(y) = 0, \psi(y) = 0, \theta(y) = 0, \phi(y) = 0 \text{ at } y = 1 \tag{40}$$

We assume the series expansion for ψ, θ, and φ as follows:

$$\psi = \psi_0(y) + \lambda\psi_1(y) + \lambda^2\psi_2(y) + \text{.....} \tag{41}$$

$$\theta = \theta_0(y) + \lambda\theta_1(y) + \lambda^2\theta_2(y) + \text{.....} \tag{42}$$

$$\phi = \phi_0(y) + \lambda\phi_1(y) + \lambda^2\phi_2(y) + \text{.....} \tag{43}$$

Substituting Eqs. (41), (42), and (43) into Eqs. (36), (37), (38), (39), and (40), and by equating the coefficients of λ^0, λ, and λ^2 and neglecting the terms of order greater than or equal to O (λ^3), the following ordinary differential equations are obtained.

$$\psi_0^{iv} - M\psi_0'' = Gr\theta_0' + Gm\phi_0' \tag{44}$$

$$\psi_1^{iv} - iu_0\psi_0'' - M\psi_1'' + iu_0''\psi_0 = Gr\theta_1' + Gm\phi_1' \tag{45}$$

$$\psi_2^{iv} - M\psi_2'' - iu_0\psi_1'' + iu_0''\psi_1 - 2\psi_0'' = Gr\theta_2' + Gm\phi_2' \tag{46}$$

$$\theta_0'' + PrDu\phi_0'' = 0 \tag{47}$$

$$\theta_1'' - iu_0 Pr\theta_0 + PrDu\phi_1'' = iPr\psi_0 T_0' \tag{48}$$

$$\theta_2'' - \theta_0 - Priu_0\theta_1 + PrDu\left(\phi_2'' - \phi_0\right) = iPr\psi_1 T_0' \tag{49}$$

$$\frac{1}{Sc}\phi_0'' + Sr\theta_0'' = 0 \tag{50}$$

$$\frac{1}{Sc}\phi_1'' + Sr\theta_1'' = iu_0\phi_0 + i\psi_0 C_0' \tag{51}$$

$$\frac{1}{Sc}\left[\phi_2'' - \phi_0\right] + Sr\left[\theta_2'' - \theta_0\right] = iu_0\phi_1 + i\psi_1 C_0' \tag{52}$$

These are subject to the following boundary conditions:

$$\psi_0' = u_0'(0), \ \psi_0 = 0, \ \theta_0 = -T_0'(0), \phi_0 = -C_0'(0) \text{ at } y = 0$$

$$\psi_0' = 0, \ \psi_0 = 0, \ \theta_0 = 0, \ \phi_0 = 0 \text{ at } y = 1$$

$$\psi_1' = 0, \psi_1 = 0, \theta_1 = 0, \phi_1 = 0, \text{ at } y = 0$$

$$\psi_2' = 0, \psi_2 = 0, \theta_2 = 0, \phi_2 = 0 \text{ at } y = 1 \tag{53}$$

Eqs. (44) through (52) are solved in sequence subject to the boundary conditions of Eq. (53), but they are not presented here for the sake of brevity.

4. Skin friction

The skin friction $\bar{\tau}_{xy}$ at any point in the fluid is given by $\bar{\tau}_{xy} = \mu\left(\frac{\partial \bar{u}}{\partial \bar{y}} + \frac{\partial \bar{v}}{\partial \bar{x}}\right)$.

The nondimensional skin friction τ_{xy} at any point is given by:

$$\tau_{xy} = \frac{d^2\bar{\tau}_{xy}}{\rho\upsilon^2} = u_0'(y) + \varepsilon e^{i\lambda x} u_1'(y) + i\varepsilon\lambda e^{i\lambda x} v_1'(y)$$

At the wavy wall $y = \varepsilon\cos\lambda x$, the coefficient of skin friction is given by:

$$\tau_\omega = \tau_{xy}]_{y=\varepsilon\cos\lambda x} = \tau_0^0 + \varepsilon Re\left[e^{i\lambda x} u_0''(0) + e^{i\lambda x} u_1'(0)\right]$$

where $\tau_0^0 = u_0'(0)$

At the flat wall y $= 1$, the coefficient of skin friction is given by:

$$\tau_1 = \tau_{xy}]_{y=1} = \tau_1^0 + \varepsilon Re\left[e^{i\lambda x} u_1'(1)\right]$$

where $\tau_1^0 = u_0'(1)$

5. Heat transfer coefficient

The nondimensional heat transfer coefficient in terms of Nusselt number Nu is given by:

$$Nu = \frac{\partial T}{\partial y} = T_0'(y) + \varepsilon\frac{\partial T_1}{\partial y} = T_0'(y) + \varepsilon e^{i\lambda x}\theta'(y)$$

At the wavy wall $y = \varepsilon\cos\lambda x$, it is as follows:

$$Nu_w = \left.\frac{\partial\theta}{\partial y}\right]_{y=\varepsilon\cos\lambda x} = T_0'(\varepsilon\cos\lambda x) + \varepsilon e^{i\lambda x}\theta'(\varepsilon\cos\lambda x)$$

$$= T_0'(0) + \varepsilon\cos\lambda x T_0''(0) + \varepsilon e^{i\lambda x}\left[\theta'(0) + \varepsilon\cos\lambda x\theta''(0)\right]$$

$$= T_0'(0) + \varepsilon\cos\lambda x T_0''(0) + \varepsilon e^{i\lambda x}\theta'(0) \ \ (\text{neglecting}\,\varepsilon^2)$$

$$= Nu_0^0 + \varepsilon Re\left[e^{i\lambda x}\left(T_0''(0) + \theta'(0)\right)\right], \ \text{where}\, Nu_0^0 = T_0'(0)$$

At the flat wall y $= 1$, the Nusselt number is represented by:

$$Nu_1 = \left.\frac{\partial\theta}{\partial y}\right]_{y=1} = T_0'(1) + \varepsilon e^{i\lambda x}\theta'(1)$$

$$= Nu_1^0 + \varepsilon Re\left[e^{i\lambda x}\theta'(1)\right], \ \text{where}\, Nu_1^0 = T_0'(1)$$

6. Mass transfer coefficient

The nondimensional mass transfer coefficient in terms of Sherwood number Sh is given by:

$$Sh = \frac{\partial C}{\partial y} = C_0(y) + \varepsilon\frac{\partial C_1}{\partial y} = C_0'(y) + \varepsilon e^{i\lambda x}\phi(y)$$

At the wavy wall $y = \varepsilon \cos \lambda x$, the Sherwood number is as follows:

$$Sh_w = \left.\frac{\partial C}{\partial y}\right]_{y=\varepsilon \cos \lambda x} = C_0' (\varepsilon \cos \lambda x) + \varepsilon e^{i\lambda x} \phi' (\varepsilon \cos \lambda x)$$

$$= C_0' (0) + \varepsilon \cos \lambda x C_0'' (0) + \varepsilon e^{i\lambda x} [\phi' (0)]$$
$$= Sh_0^0 + \varepsilon Re \left[e^{i\lambda x} (C_0'' (0)) + \phi' (0)\right]$$

where: $Sh_0^0 = C_0' (0)$

At the flat wall y = 1, the Sherwood number is defined by:

$$Sh_1 = \left.\frac{\partial C}{\partial y}\right]_{y=1} = C_0' (1) + \varepsilon e^{i\lambda x} \phi' (1) = Sh_1^0 + \varepsilon Re \left[e^{i\lambda x} \phi' (1)\right]$$

where $Sh_1^0 = C_0' (1)$

7. Results and discussion

In order to get physical insight into the problem, we have carried out numerical calculations for nondimensional velocity field, temperature field, species concentration field, and skin frictions at the walls by assigning some specific values to the parameters entering into the problem and the effects of these values on the above fields are demonstrated graphically. In our investigation the values of the parameter λ (frequency parameter) and ε (amplitude parameter) are kept fixed at 0.001 and 0.01, respectively, and the values of the other parameters are chosen arbitrarily.

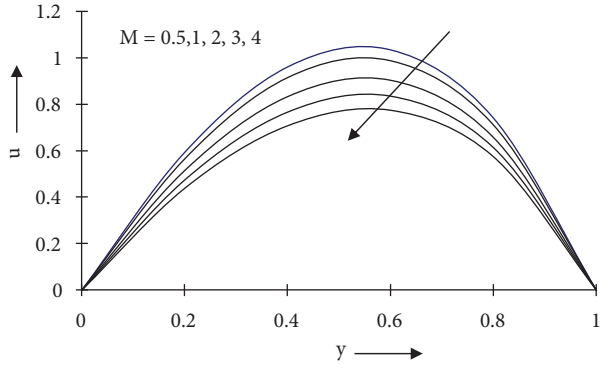

Figure 1. Velocity versus y under M for Pr = 0.71, Du = 0.2, Sc = 0.6, Sr = 1, $\alpha = 1$, Gr = 2, Gm = 2, m = 5, n = 1, $\lambda = 0.001$, $\varepsilon = 0.01$.

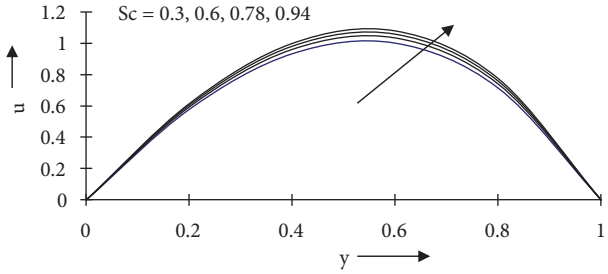

Figure 2. Velocity versus y under Sc for Pr = 0.71, Du = 0.2, Sr = 1, $\alpha = 1$, M = 0.5, Gr = 2, Gm = 2, m = 5, n = 1, $\lambda = 0.001$, $\varepsilon = 0.01$.

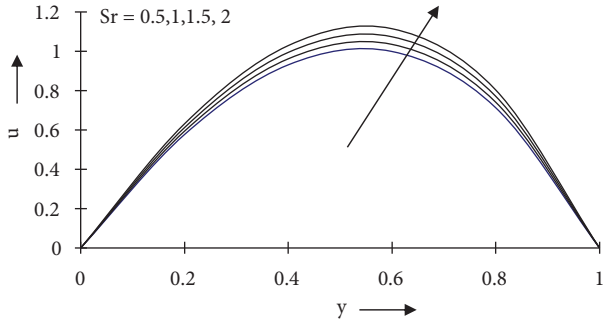

Figure 3. Velocity versus y under Sr for Pr = 0.71, Du = 0.2, Sc = 0.6, $\alpha = 1$, M = 0.5, Gr = 2, Gm = 2, m = 5, n = 1, $\lambda = 0.001$, $\varepsilon = 0.01$.

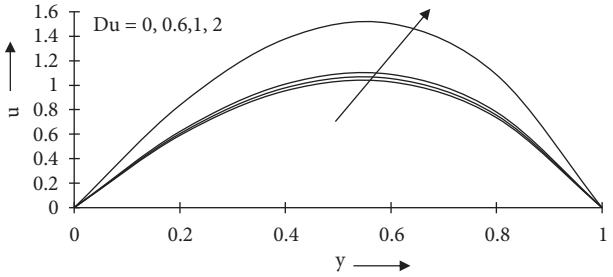

Figure 4. Velocity versus y under Du for Pr = 0.71, Sc = 0.6, Sr = 1, $\alpha = 1$, M = 0.5, Gr = 2, Gm = 2, m = 5, n = 1, $\lambda = 0.001$, $\varepsilon = 0.01$.

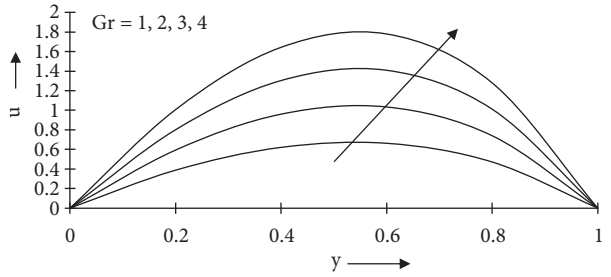

Figure 5. Velocity versus y under Gr for Pr = 0.71, Du = 0.2, Sc = 0.6, Sr = 1, $\alpha = 1$, M = 0.5, Gm = 2, m = 5, n = 1, $\lambda = 0.001$, $\varepsilon = 0.01$.

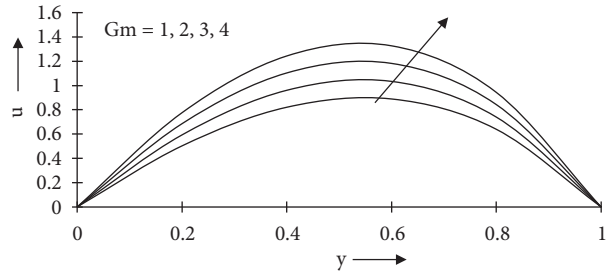

Figure 6. Velocity versus y under Gm for Pr = 0.71, Du = 0.2, Sc = 0.6, Sr = 1, $\alpha = 1$, M = 0.5, Gr = 2, m = 5, n = 1, $\lambda = 0.001$, $\varepsilon = 0.01$.

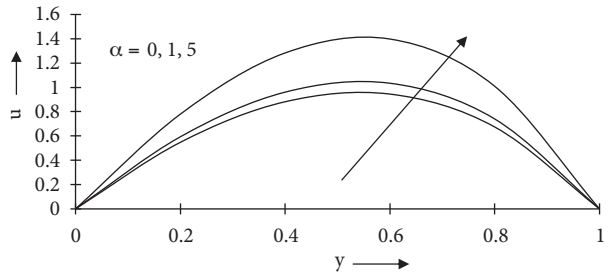

Figure 7. Velocity versus y under α for Pr = 0.71, Du = 0.2, Sc = 0.6, Sr = 1, M = 0.5, Gr = 2, Gm = 2, m = 5, n = 1, $\lambda = 0.001$, $\varepsilon = 0.01$.

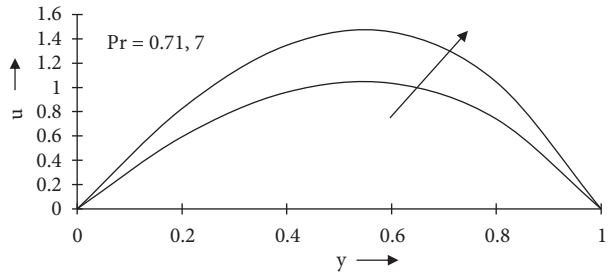

Figure 8. Velocity versus y under Pr for Du = 0.2, Sc = 0.6, Sr = 1, $\alpha = 1$, M = 0.5, Gr = 2, Gm = 2, m = 5, n = 1, $\lambda = 0.001$, $\varepsilon = 0.01$.

Figures 1–8 represent the variation of the velocity field u versus y under the effects of Hartmann number M, Schmidt number Sc, Soret number Sr, Dufour number Du, thermal Grashof number Gr, solutal Grashof number Gm, heat-generating source α, and Prandtl number Pr. From these figures we observe that the velocity field increases as Sc, Sr, Du, Gr, Gm, α, and Pr increase and decreases as M increases. This indicates the fact that the fluid motion is retarded due to application of the transverse magnetic field and mass diffusion, whereas it is accelerated under the effects of thermal–diffusion, diffusion–thermo, buoyancy forces (thermal and solutal), heat-generating source, and increasing Prandtl number. These figures further show that the velocity profiles exhibit a parabolic nature within the channel and the maximum velocity is attained at the middle of the channel.

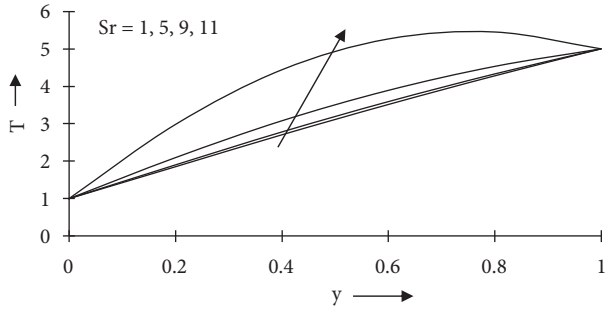

Figure 9. Temperature versus y under Sr for Pr = 0 .71, Du = 0.2, Sc = 0.6, α =1, M = 0.5, Gr = 2, Gm = 2, m = 5, n = 1, λ = 0.001, ε = 0.01.

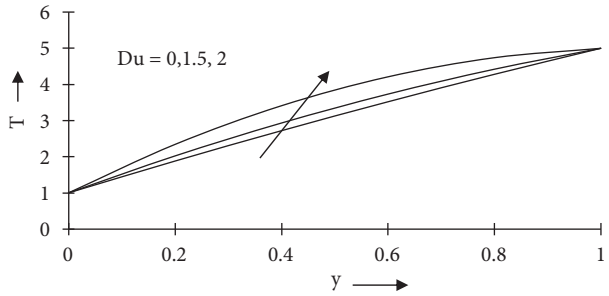

Figure 10. Temperature versus y under Du for Pr = 0.71, Sc = 0.6, Sr = 1, α = 1, M = 0.5, Gr = 2, Gm = 2, m = 5, n = 1, λ = 0.001, ε = 0.01.

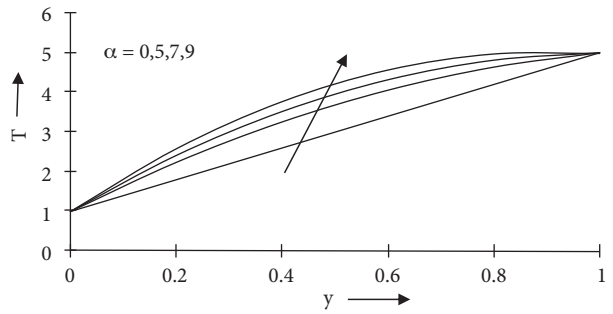

Figure 11. Temperature versus y under α for Pr = 0.71, Du = 0.2, Sc = 0.6, Sr = 1, M = 0.5, Gr = 2, Gm = 2, m = 5, n = 1, λ = 0.001, ε = 0.01.

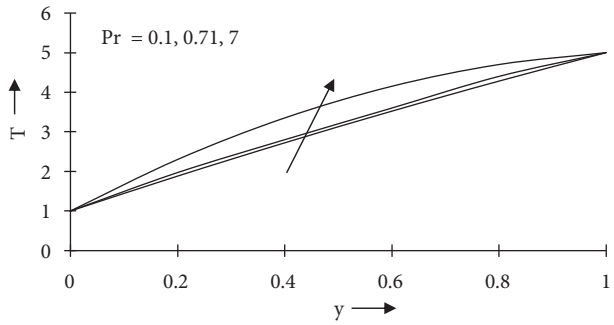

Figure 12. Temperature versus y under Pr for Du = 0.2, Sc = 0.6, Sr = 1, α = 1, M = 0.5, Gr = 2, Gm = 2, m = 5, n = 1, λ = 0.001, ε = 0.01.

Figures 9–12 exhibit the behavior of the temperature field against y under the influence of parameters Sr, Du, α, and Pr. It is inferred from these figures that an increase in the values of each of the above parameters causes the fluid temperature to rise up slowly and steadily. This phenomenon is clearly supported from physical reality as thermal–diffusion, diffusion–thermo, heat-generating source, and increasing Prandtl number always have a tendency to raise the fluid temperature significantly.

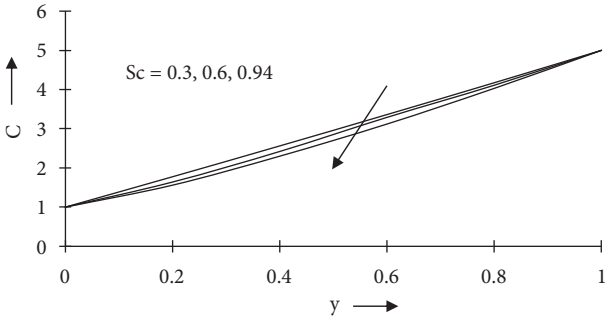

Figure 13. Concentration versus y under Sc for Pr = 0.71, Du = 0.2, Sr = 1, α = 1, M = 0.5, Gr = 2, Gm = 2, m = 5, n = 5, λ = 0.001, ε = 0.01.

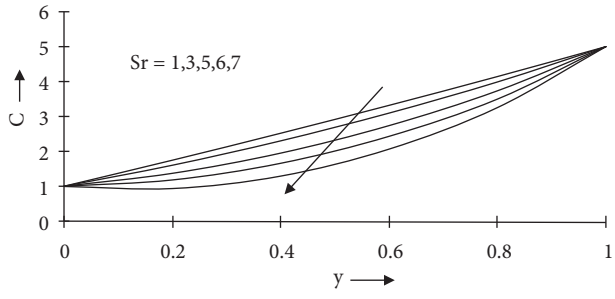

Figure 14. Concentration versus y under Sr for Pr = 0.71, Du = 0.2, Sc = 0.6, α = 1, M = 0.5, Gr = 2, Gm = 2, m = 5, n = 5, λ = 0.001, ε = 0.01.

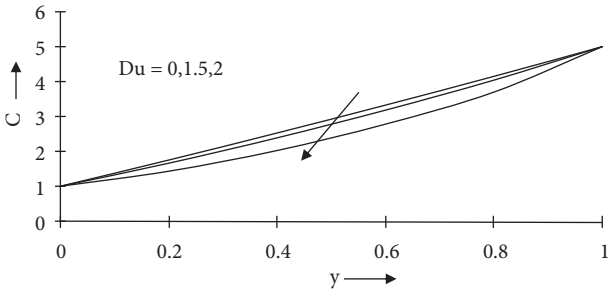

Figure 15. Concentration versus y under Du for Pr = 0.71, Sc = 0.6, Sr = 1, α = 1, M = 0.5, Gr = 2, Gm =2, m = 5, n = 5, λ = 0.001, ε = 0.01.

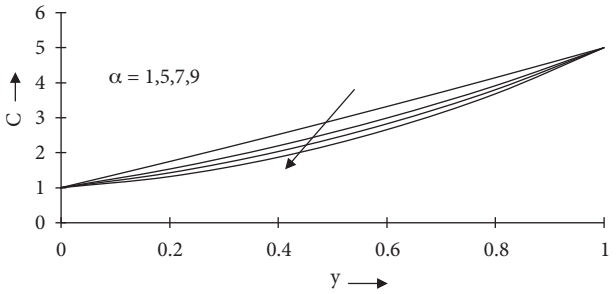

Figure 16. Concentration versus y under α for Pr = 0.71, Du = 0.2, Sc = 0.6, Sr = 1, M = 0.5, Gr = 2, Gm = 2, m = 5, n = 5, λ = 0.001, ε = 0.01.

The variation of species concentration C versus y under the influence of Schmidt number Sc, Soret number Sr, Dufour number Du, and heat-generating source α is presented in Figures 13–16. These figures indicate that the concentration level of the fluid falls due to increasing values of Schmidt number, Soret number, Dufour number, and heat source parameter. In other words, the thickness of the concentration boundary layer falls under the effects of thermal–diffusion (Soret effect), diffusion–thermo (Dufour effect), and heat-generating source, whereas the mass diffusion results in an increase of the thickness of the concentration boundary layer. These observations are consistent with the physics of the problem.

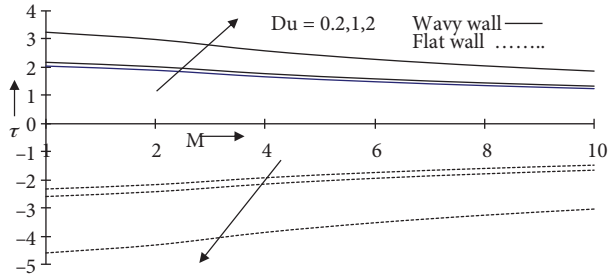

Figure 17. Skin friction τ versus M under Du for Pr = 0.71, Sc = 0.6, Sr = 1, α = 1, Gr = 2, Gm = 2, m = 5, n = 1, λ = 0.001, ε = 0.01, $\lambda x = \pi/2$.

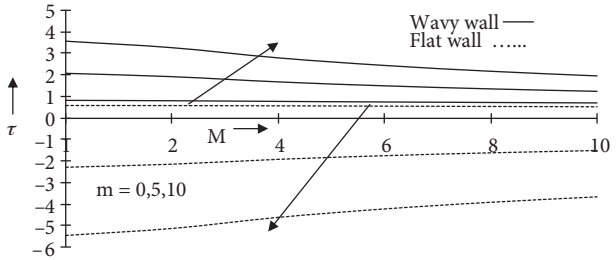

Figure 18. Skin friction τ versus M under m for Pr = 0.71, Du = 0.2, Sc = 0.6, Sr = 1, α = 1, Gr = 2, Gm = 2, n = 1, λ = 0.001, ε = 0.01, $\lambda x = \pi/2$.

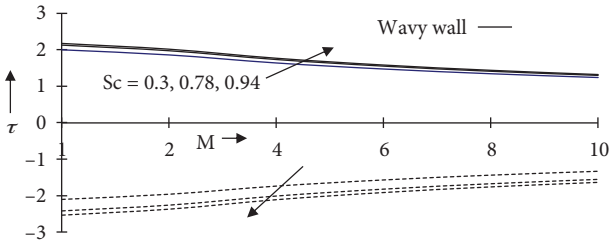

Figure 19. Skin friction τ versus M under Sc for Pr = 0.71, Du = 0.2, Sr = 1, α = 1, Gr = 2, Gm = 2, m = 5, n = 1, λ = 0.001, ε = 0.01, $\lambda x = \pi/2$.

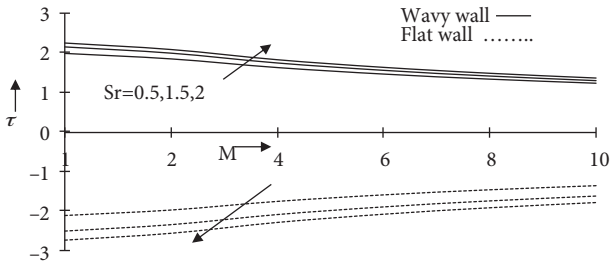

Figure 20. Skin friction τ versus M under Sr for Pr = 0.71, Du = 0.2, Sc = 0.6, α = 1, Gr = 2, Gm = 2, m = 5, n = 1, λ = 0.001, ε = 0.01, $\lambda x = \pi/2$.

The nature of skin friction τ at both the wavy wall and the flat wall is demonstrated in Figures 17–20. It is clear from Figures 17, 18, and 20 that the magnitudes of the viscous drag at both the walls rise up under

the influence of Dufour effect, increasing wall temperature ratio and Soret effect. A reverse trend of behavior of τ in the case of mass diffusion is marked in figure 19.

8. Conclusions

1. The fluid motion is retarded under the application of the transverse magnetic field and accelerated due to thermal–diffusion and diffusion–thermo effects.

2. An increase in Soret number and Dufour number leads the fluid temperature to increase.

3. The thickness of the concentration boundary layer decreases under Soret and Dufour effects.

4. The thermal–diffusion and diffusion–thermo effects lead the magnitude of the viscous drag at the wavy wall and at the flat wall to increase.

5. Finally, it is concluded that the thermal–diffusion and diffusion–thermo effects have a significant role in controlling the flow and transport characteristics.

Nomenclature

g	Acceleration due to gravity
ε	Amplitude parameter
$\overline{x}, \overline{y}$	Cartesian coordinates
μ	Coefficient of viscosity
β	Coefficient of volume expansion for heat transfer
C_s	Concentration susceptibility
D_M	Coefficient of mass diffusion
Q	Constant heat addition/absorption
d	Distance between 2 walls
ρ_s	Density of the fluid in static condition
Du	Dufour number
σ	Electrical conductivity
$\overline{p}$	Fluid pressure
ρ	Fluid density
λ	Frequency parameter
$\overline{T}$	Fluid temperature
$\overline{T_s}$	Fluid temperature in static condition
Gr	Grashof number for heat transfer
Gm	Grashof number for mass transfer
α	Heat source parameter
υ	Kinematic viscosity
T_m	Mean fluid temperature
M	Magnetic parameter
$\overline{p}_s$	Pressure of the fluid in static condition
Pr	Prandtl number
$\overline{B}$	Strength of the applied magnetic field
$\overline{C}$	Species concentration
C_p	Specific heat at constant pressure
$\overline{C}_\omega$	Species concentration at the wavy wall
$\overline{C}_1$	Species concentration at the flat wall
Sr	Soret number
Sc	Schmidt number
k	Thermal conductivity
$\overline{T}_\omega$	Temperature of the wavy wall
$\overline{T}_1$	Temperature of the flat wall
K_T	Thermal diffusion ratio
$\overline{u}, \overline{v}$	Velocity components
$\overline{\beta}$	Volumetric coefficient of expansion with species concentration
m	Wall temperature ratio
n	Wall concentration ratio

Acknowledgment

The corresponding author is highly thankful to CSIR-HRDG for funding this research work under Research Grant-in-Aid No. 25(0209)/12/EMR-II.

References

[1] Lekoudis, S. G.; Nayfeh, A. H.; Saric, W.S. *Phys. Fluids* **1976**, *19*, 514–519.

[2] Shankar, P. N.; Sinha, U. N. *J. Fluid Mech.* **1976**, *77*, 243–256.

[3] Lessen, M.; Gangwani, S. T. *Phys. Fluids* **1976**, *19*, 510–513.

[4] Vajravelu, K; Sastri, K. S. *J. Fluid Mech.* **1978**, *86*, 365–383.

[5] Rao, C. N. B.; Sastri, K. S. *Ind. J. Maths. & Math. Sci.* **1982**, *5*, 585–594.

[6] Vajravelue, K; Sastri, K. S. *Int. J. Heat Mass Trans.* **1980**, *23*, 408–411.

[7] Rao, C. N. B. *Rev. Roum. Phys. Tonu.* **1982**, *27*, 783–799.

[8] Das, U. N.; Ahmed, N. *Ind. J. Pure Appl. Math.* **1992**, *23*, 295–304.

[9] Eckert, E. R. G.; Drake, R. M. *Analysis of Heat and Mass Transfer*; McGraw-Hill: New York, 1972.

[10] Dursunkaya, Z.; Woret, W. M. *Int. J. Heat Mass Trans.* **1992**, *35*, 2060–2065.

[11] Kafoussias, N. G.; Williams, E. M. *Int. J. Eng. Sci.* **1995**, *33*, 1369–1376.

[12] Sattar, M. A.; Alam, M. M. *Indian J. Pure Appl. Math.* **1994**, *25*, 679–688.

[13] Alam, M. S.; Rahman, M.; Maleque, A.; Ferdows, M. *Tham. Int. J. Sci. Tech.* **2006**, *11*, 1–12.

[14] Raju, M. C.; Varma, S. V. K.; Reddy, P. V.; Saha, S. *J. of Mech. Eng. ME* **2008**, *39*, 65–70.

[15] Srinivasacharya, D.; RamReddy, Ch. *Nonlinear Anal. Model. Control* **2011**, *16*, 100–115.

[16] Srinivasacharya, D.; RamReddy, Ch. *Adv. Appl. Math. Mech.* **2011**, *3*, 389–400.

[17] Srinivasacharya, D.; RamReddy, Ch. *Heat Trans. Asian Res.* **2013**, *42*, 111–124.

[18] Ostrach, S. *NACA Tech. Note* **1952**, 2863.